

## **CHAPTER 5: THE SOUTPANSBERG GROUP.**

Outcrops of the Soutpansberg Group within the study area can be classified within two formations: The Sibasa Formation and the Wyllies Poort Formation. The outcrop of the Sibasa Formation is limited to the western edge of Blouberg Mountain, and the Wyllies Poort Formation outcrops extensively in the northeastern part of the study area. Both formations only underlie areas to the north of the southern strand of the Melinda Fault. There is also an isolated outcrop of the Wyllies Poort Formation in the north western part of the study area, at around 23°06'S; 28°33'E (Appendix 1).

### **5.1: The Sibasa Formation:**

Outcrops discussed in this section consist of an amygdaloidal rock that is usually highly weathered (Figures 5.1 and 5.2). The lithology is generally poorly exposed, though outcrops can be found on the lower slopes of Sesuane hill (23°07.5'S; 28°51.5'E) beneath the quartzites of the Wyllies Poort Formation, 6km west of this location, under the eastern slopes of Lebu hill, and also on the upper slopes of a deep valley at around 23°07.5'S; 28°54.50'E. Despite the poor outcrop and generally weathered nature of the rock, the presence of amygdales (Figure 5.1) and locally ropey texture (Figure 5.2), provides good evidence that the Sibasa Formation predominantly consists of lava flows. Three samples of lava were collected, one from each of these locations, and prepared for I.C.P.M.S. and X.R.F. analysis (both major and trace elements). The results from these analyses of the three lavas are shown in Table 5.1.

A plot of the weight percent of total alkalis ( $\text{Na}_2\text{O} + \text{K}_2\text{O}$ ; Table 5.1) against silica of lavas from each of these three locations is shown in Figure 5.3, and shows that the lavas can be classified as basalt. Figure 5.3 also shows the plot of total alkalis against silica from previously published analyses (Crow and Condie, 1990) from Sibasa basalts outcropping in the Soutpansberg mountains to the east (Figure 1.7). Figure 5.3 demonstrates that lavas from the Blouberg area compare favourably with the composition of Sibasa basalts from elsewhere in the Soutpansberg basin. The basaltic/basaltic andesite

classification for the lavas is in contrast to the trachyandesitic composition for the same lithology, proposed by Jansen (1976) and Meinster (1977). They named the lavas as the “My Darling trachyandesitic Member” of the Blouberg Formation (Jansen, 1976) or the “My Darling lava Formation” of the pre-Blouberg Lebu Complex (Meinster, 1977). The basaltic composition presented here, and the fact that mapping shows that these basalts can only be seen to be overlain by the Wyllies Poort Formation (Appendix 1), agree with the proposal by Brandl (1986b) that the rocks rather correlate with the Sibasa Formation of the Soutpansberg Group. Even though elements K and Na are considered to be highly mobile, and may be of limited use in characterising ancient rocks, samples analysed were fresh, and such methods have been similarly successfully applied to other Precambrian volcanic rocks (e.g. Harmer and von Gruenewaldt, 1991). In thin section, these Sibasa basalts can be seen to be comprised of small phenocrysts of olivine (often replaced by serpentine), in a groundmass of plagioclase laths and augite (Figure 5.4).

Incompatible trace element data are also presented in Table 5.1. A plot of incompatible trace elements is shown in Figure 5.5, and shows relative enrichment of incompatible trace elements, with negative anomalies of Nb, P and Ti. Further discussion of the trace element chemistry of the Sibasa lavas will be given in Chapter 8, where these data will be compared with incompatible trace element data from dolerite dykes swarms intruding the Blouberg Formation and the Waterberg Group strata.

## **5.2: The Wyllies Poort Formation:**

Strata of the Wyllies Poort Formation occupy the northern part of the study area, and underlie areas only to the north of the southern strand of the Melinda Fault (Appendix 1). Generally the Wyllies Poort Formation underlies the mountainous areas of Blouberg mountain and its foothills to the northeast, though the unit also outcrops in the north-western part of the study area (Appendix 1).

The strata are generally purple/brown quartzites, which locally contain thin pebble washes, about 3-10cm thick (Figure 5.6). Pebbles are composed of quartz, quartzite and,

rarely, coarse-grained sandstone, and are generally 1-2cm in diameter. Locally, the Wyllies Poort Formation is less recrystallised, and can be seen to be composed, generally, of medium- to coarse-grained sandstone, consisting of sub-angular to sub-rounded quartz and lithic (quartzite) grains with high sphericity. Locally these grains may reach up to 2mm in diameter (i.e small granules).

The mountainous terrain underlain by the Wyllies Poort Formation offers good topography over which architectural relationships can be easily traced from photographs. The Wyllies Poort Formation appears to be comprised of architectural elements of major sandstone sheets (element CHS; Table 3.1). Individual channel forms, so conspicuous in other clastic strata in the Blouberg area, are absent in the Wyllies Poort Formation (Figure 5.7).

The Wyllies Poort Formation has a maximum preserved thickness of about 700m, from its lower contact with the basement, Sibasa Formation or Mogalakwena Formation in the Blouberg mountain foothills, to the summit (Appendix 1). The generally steep nature of the topography around Blouberg mountain provides few accessible opportunities for recording vertical changes in facies characteristics throughout the succession. However, the line marked in Figure 5.8 follows a relatively safe footpath from the lower-most outcrops of the Wyllies Poort Formation to the summit. The following data describe the general vertical facies changes recorded from this area.

The lower-most 200m of the Wyllies Poort Formation are comprised of trough cross-bedded coarse sandstone facies (St; Table 3.1) with relatively small sets, consisting of moderately sorted, sub-rounded to sub-angular quartz grains and lithic clasts (quartzite). Quartz grains are commonly less than 1mm in diameter, though lithic clasts rarely reach more than 2mm in diameter (granules). Set thicknesses generally vary between 5 and 40cm (Figure 5.9). Soft-sedimentary deformation structures can be found locally (Figure 5.9). Cosets are up to 150cm in thickness. Pebbles are common in this lower-most portion of the Wyllies Poort strata, deposited either on bedding or foreset planes, and help define fining-upwards foreset laminae/beds.

Above the cross-bedded facies, strata consist of planar-bedded sandstone facies (Sh; Table 3.1), where beds are commonly 5-10cm thick. Again, patches which are less recrystallised appear to be composed of sub-angular to sub-rounded quartz grains up to 2mm in diameter, with similarly-sized lithic clasts (quartzitic). Parting lineation was not recorded on planar beds, though it may have been destroyed during recrystallisation if originally present. Locally, sets of very low-angled ( $<10^0$ ) cross-bedding (facies Sl; Table 3.1) can be seen between the planar bedded facies. Bedding surfaces are locally ripplemarked (Facies Sr; Table 3.1), including symmetrical ripples (Figure 5.10), linguoid ripples (Figure 5.11) and asymmetric ripples (Figure 5.12). Together these three facies make up about 200m of the Wyllies Poort succession, and are devoid of pebbles.

Above this, about for about 300m vertically, a sandstone facies (composed of quartz grains and quartzitic lithic clasts) with large-scale trough cross-beds (St) is dominant. Again, pebble conglomerate interbeds are rare. Trough cross-bed sets are commonly between 1 and 2m in thickness; they are locally bound above and below by planar-bedded sandstone (Figure 5.13). Rarely, very low angled planar cross-bedding is also present, interbedded with the large scale trough cross-bedded facies (Figure 5.13). Locally, soft-sediment deformation is indicated by the presence of sand volcanoes (Figure 5.14). On the summit plateau of Blouberg mountain (the very top of the preserved section), there is a return to planar-bedded, ripplemarked sandstone facies (Sr; Table 3.1).

Thus the Wyllies Poort Formation can be considered to contain two dominant facies associations; (1.) small-and large-scale trough cross-bedded sandstones with interbedded pebble conglomerate, and (2.) planar-bedded sandstones with ripplemarks and low-angled (planar) cross-beds.

Wyllies Poort quartzite appears to have undergone intense pressure solution of grain boundaries, as shown by thin section in Figure 5.15, so that original textures are difficult to recognise. Areas which have undergone less pressure solution, and hence less recrystallisation, can be seen to be made up of sub-rounded to angular grains of quartz, with rare lithic clasts of quartzite (Figure 5.16), and grains appear to have quartz

overgrowths. Counting of 500 points from 1 section within the Wyllies Poort quartzites produced an average composition of 73% quartz grains and 27% lithic fragments, so they can be classified as lithic arenites (Pettijohn *et al.*, 1973). Recorded lithic fragments were quartzitic and, rarely, very fine sandstone.

Recorded pebbles within the Wyllies Poort Formation were generally quartz or quartzitic, though locally pebbles of coarse sandstone were found. A thin section of one of these sandstone pebbles is shown in Figure 5.17, and shows that interstitial red clays support the grains in the pebble. The composition of one of these sandstone pebbles was determined by point counting, and a survey of 500 points gave an average composition of 48% quartz grains, 25% lithic fragments (quartzite), and 27% interstitial matrix (red clay minerals). Thus, using the scheme of Pettijohn *et al.* (1973), ordinarily used to discriminate arenites, the sandstone pebbles can be characterised as having a lithic wacke composition. The thin section shown in Figure 5.18 is from a coarse-grained sandy sheet in the Mogalakwena Formation (Section 4.41) and closely resembles that of the coarse sandstone pebble shown in Figure 5.17. A point count from this Mogalakwena thin section showed an average composition (from 500 points) of 40% quartz, 39% matrix (=clays) and 21% lithic fragments (=quartzite), which compares favourably with the point count from the Wyllies Poort-hosted sandstone pebble.

Palaeocurrent directions recorded in the Wyllies Poort Formation are shown in Figure 5.19, and show that different facies recorded in the Wyllies Poort Formation generally show contrasting palaeocurrent directions. Large- and small-scale trough cross-bedded sandstones, recorded from the area shown on Figure 5.8, are given in Figure 5.19a. Ripplemarked sandstones (both asymmetric and symmetric) from the same area, associated with planar-bedded sandstone are shown in Figures 5.19b and 5.19c, respectively. Palaeocurrent directions measured from ripplemarked sandstones recorded in the north eastern foothills of Blouberg (at around 23°00'S; 29°07'E) are shown in Figure 5.19d.



**Figure 5.1: Amygdaloidal basalt of the Sibasa Formation at 23°06.68'S; 28°52.32'E. Hammer is 30cm long.**



**Figure 5.2: Ropey lava texture in basalt of the Sibasa Formation at 23°06.68'S; 28°52.32'E. Hammer is 30cm long.**



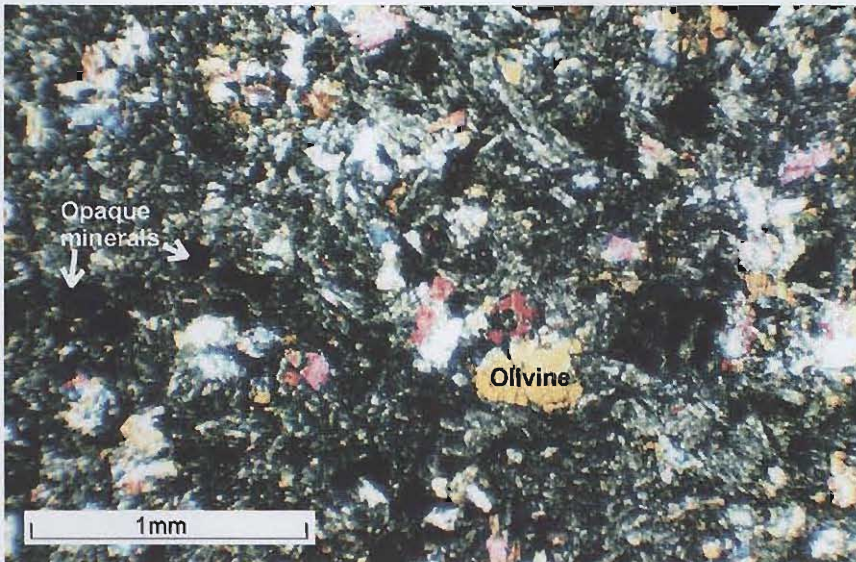


**Figure 5.4: Photomicrograph of Sibasa basalt, showing olivine phenocrysts in a groundmass of plagioclase feldspar and augite. Several opaque minerals are also present.**

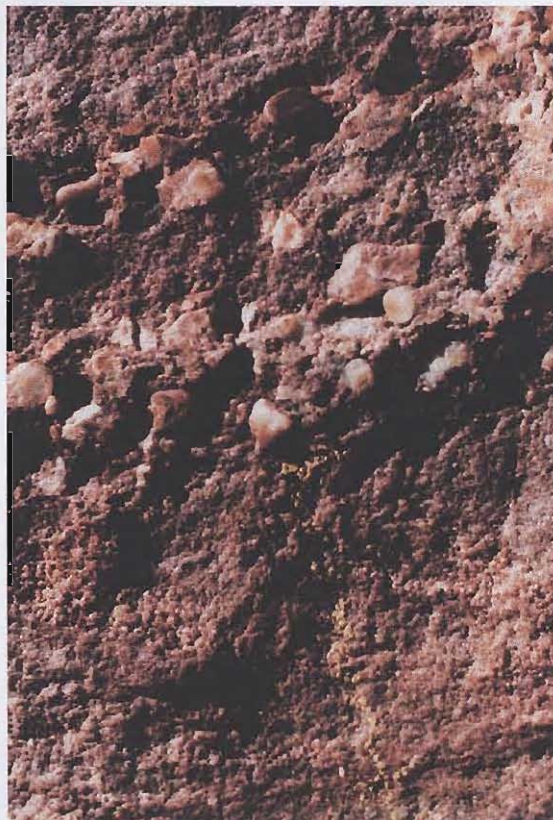


**Figure 5.6: Thin layer of quartz pebbles in the Wyllies Poort Formation. Pebble layer is interbedded with brown/purple quartzite typical of the Wyllies Poort Formation. Section is 20cm high.**

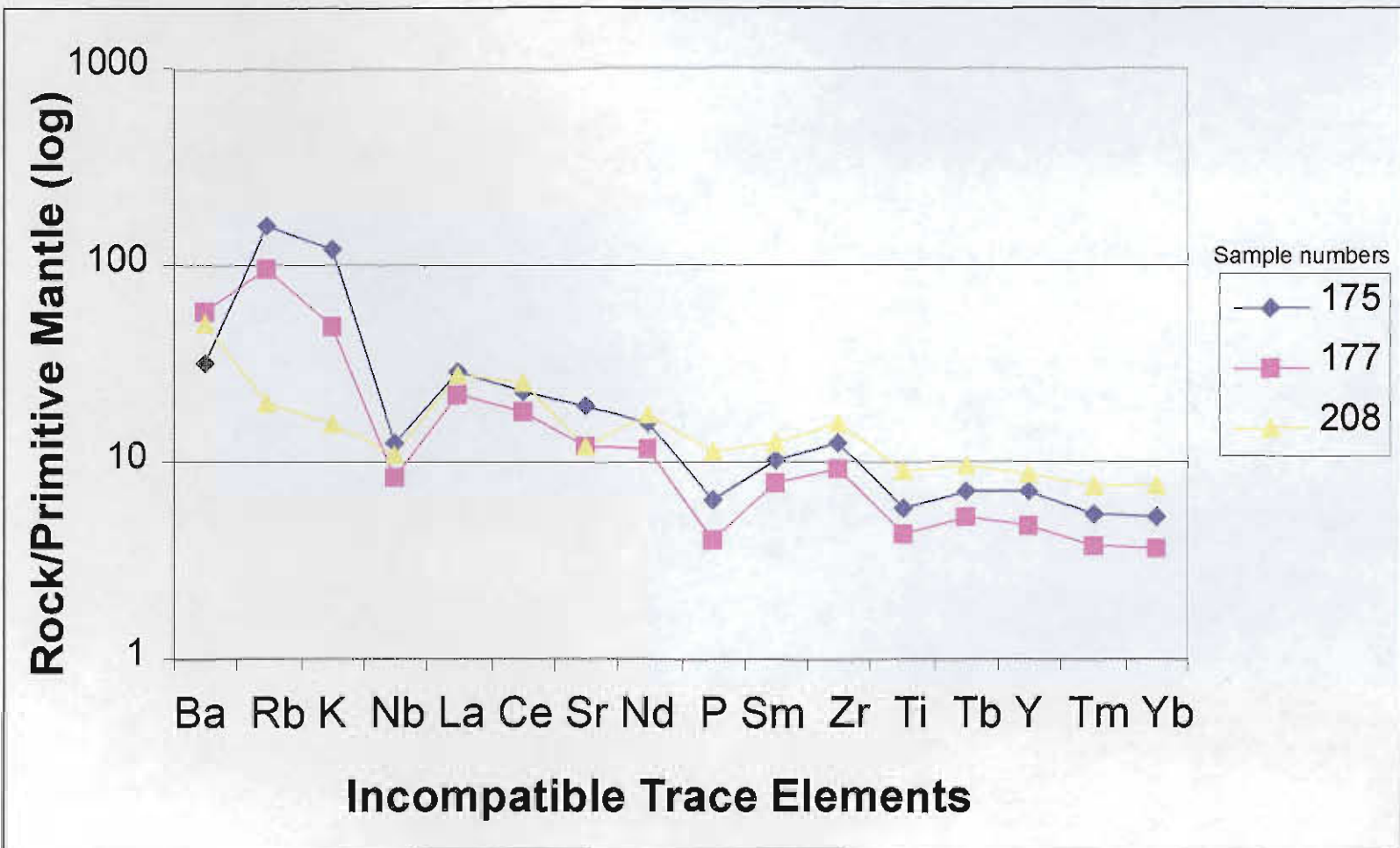
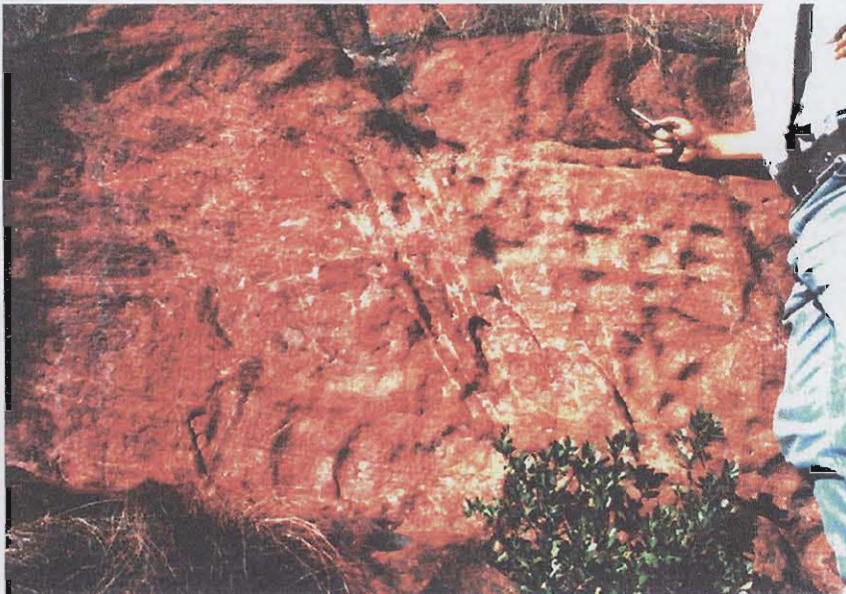


Figure 5.5: Spidergram to show values of normalised incompatible trace element values determined for the Sibasa Formation.



**Figure 5.7: Oblique aerial photograph of the summit area of Blouberg mountain, showing relatively horizontally inclined sheet-like elements with no channel forms preserved.**



**Figure 5.9: Relatively small (20cm set thickness) trough cross-bedded sets in the lower part of the Wyllies Poort Formation. The indicated foresets have been overturned during soft sedimentary deformation, possibly caused by strong water currents during the deposition of subsequent beds.**

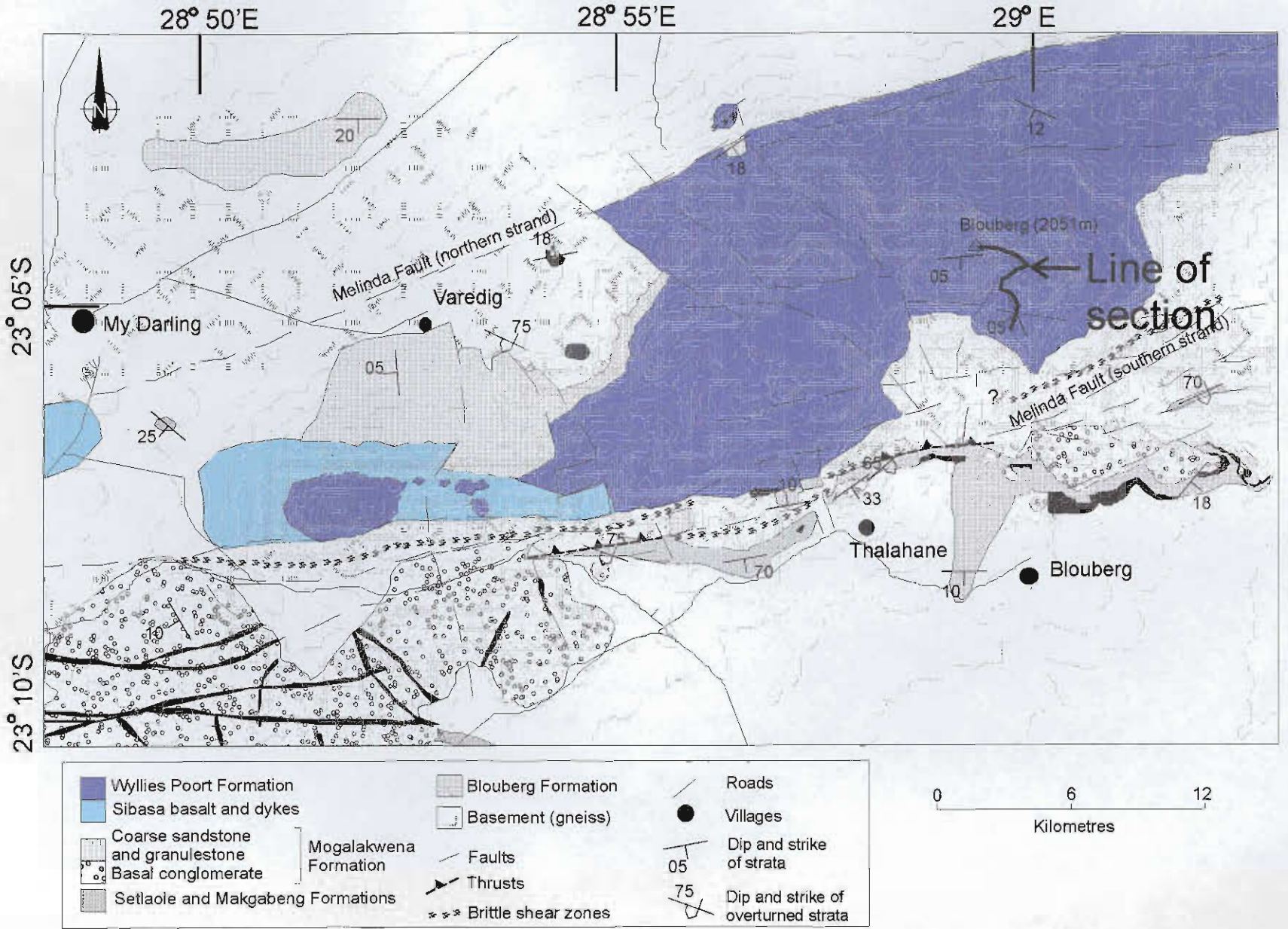


Figure 5.8: Location of stratigraphic section recorded in the Wyllies Poort Formation.



**Figure 5.10: Large symmetric ripples in the mid-Wyllies Poort Formation at 23°04.57'S; 28°59.65'E. Hammer is 30cm long.**



**Figure 5.11: Linguoid ripples in the upper strata of the Wyllies Poort Formation. Recorded at 23°04.26'S; 28°59.19'E. Lens cap is 5cm wide.**



**Figure 5.12: Asymmetric ripplemarks in the Wyllies Poort Formation at 22°59.67'S; 29°09.58'E. Lens cap is 5cm wide.**

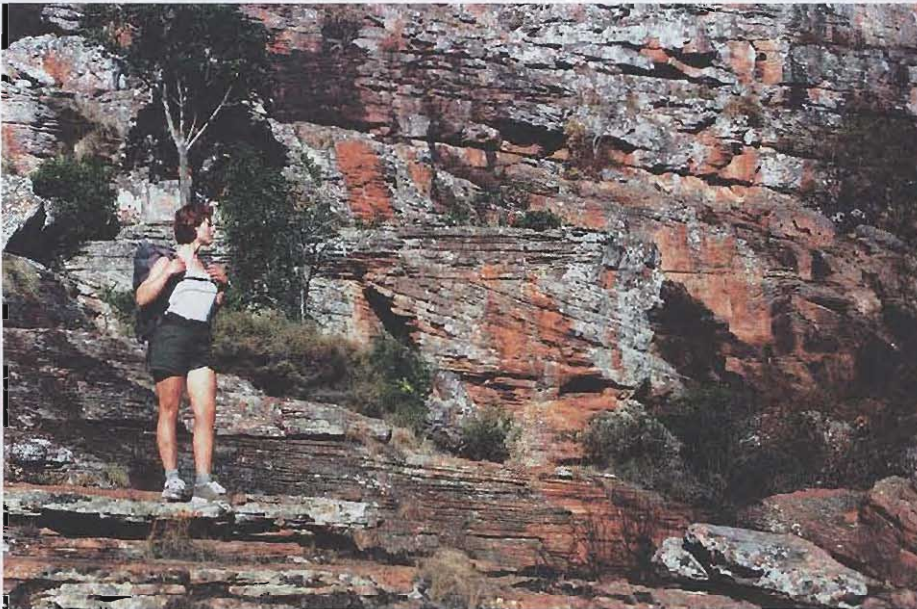


**Figure 5.13: Large scale (>2m) trough cross-bedded sandstone (middle distance), interbedded with planar-bedded sandstone and rare very low angle (<10°) planar cross-bedded sandstone (foreground), in the mid-Wyllies Poort Formation. Recorded at 23°04.57'S; 28°59.65'E.**



**Figure 5.14: Plan section of a sand volcano, developed in the mid-Wyllies Poort Formation at 23°04.25'S; 28°59.52'E. Lens cap is 5cm wide.**

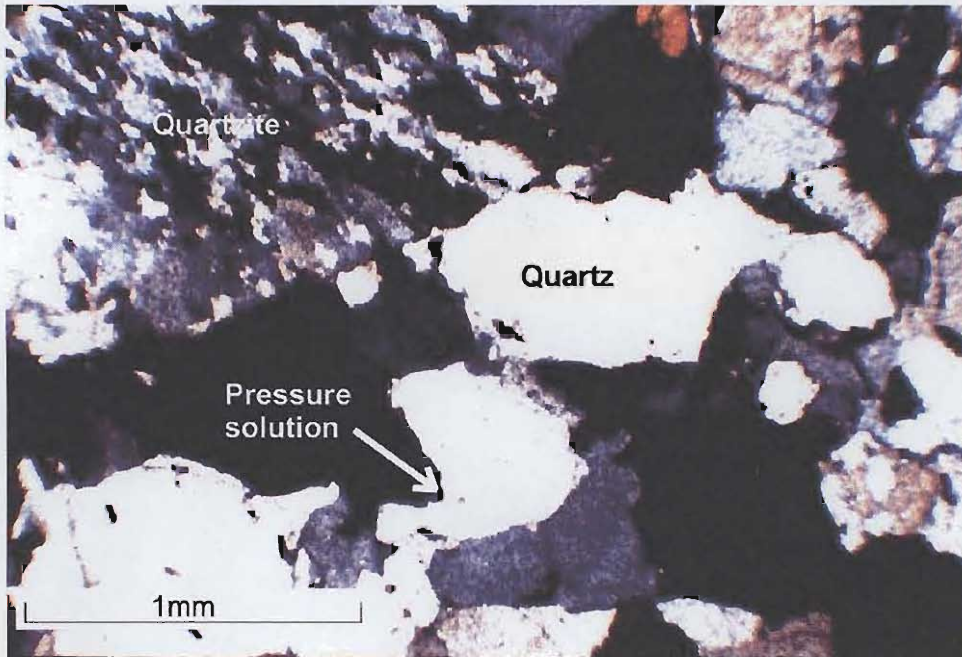


**Figure 5.15: Photomicrograph of Wyllies Poort quartzite, showing pressure solution at boundaries of quartz and lithic grains (quartzite).**

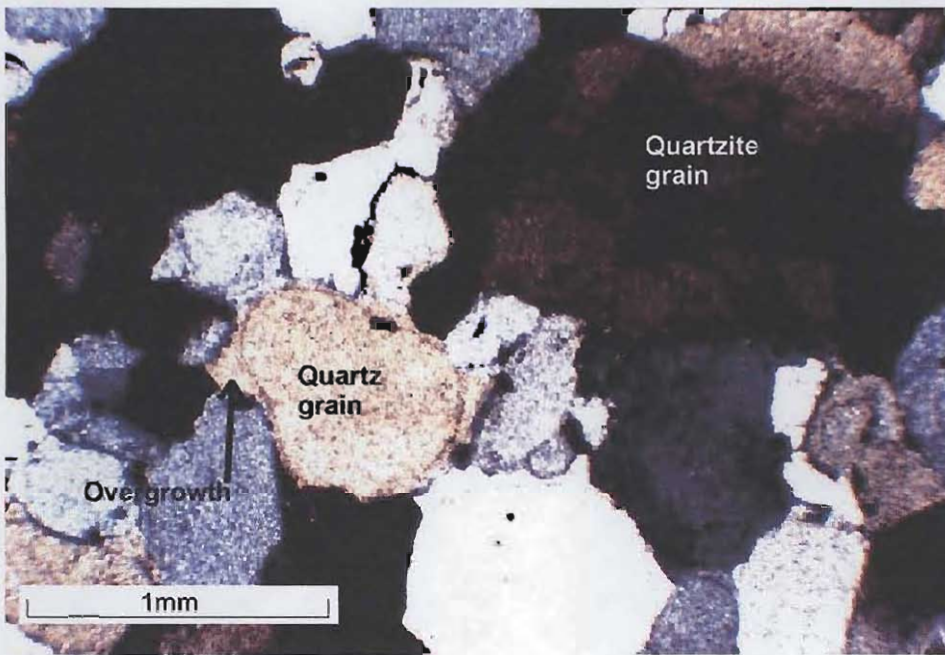


Figure 5.16: Photomicrograph of Wyllies Poort sandstone, showing sub-rounded to sub-angular grains with quartz overgrowths in optical continuity with parent grains of quartz and quartzite.

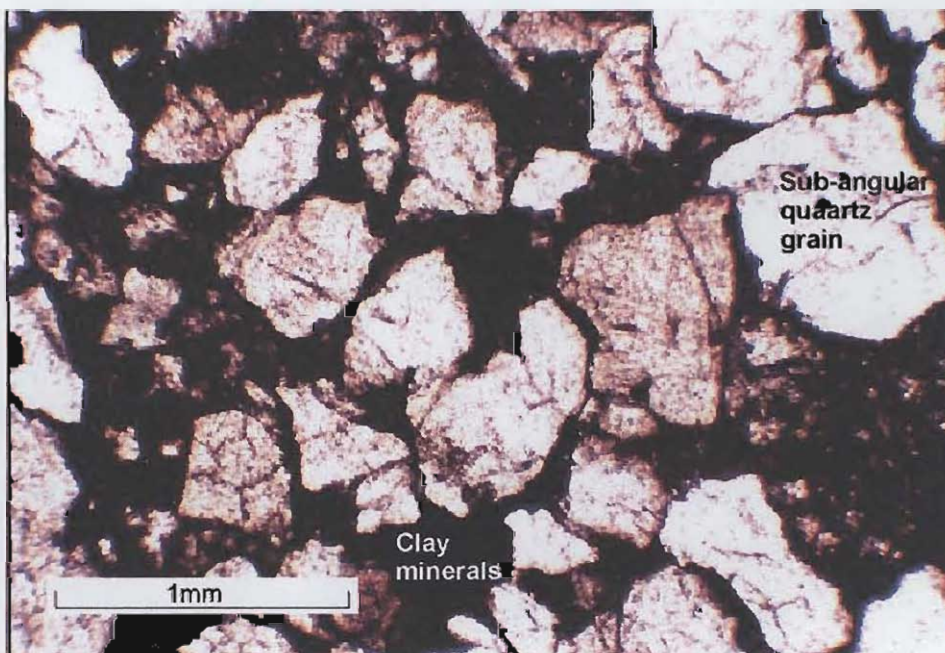
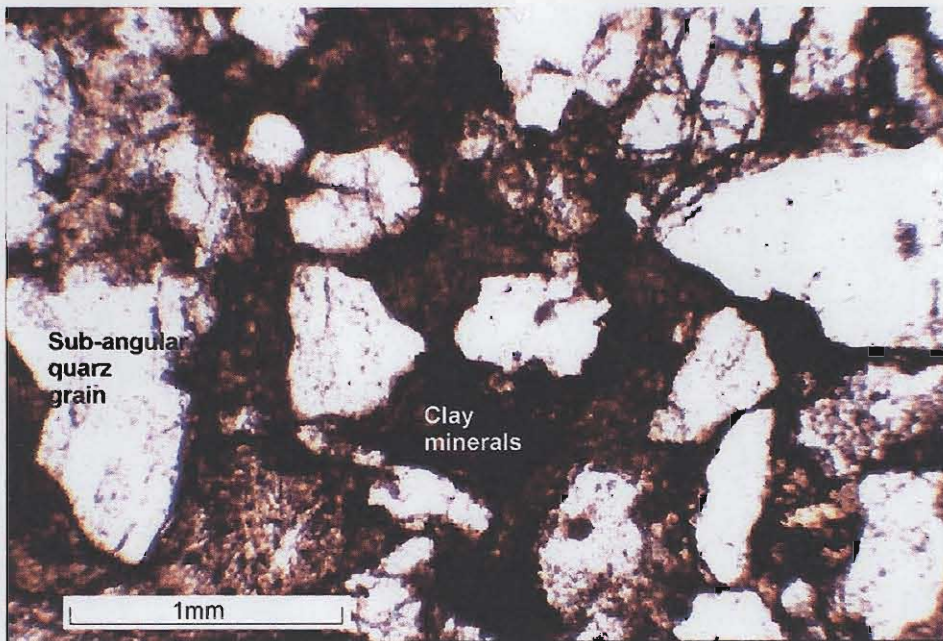
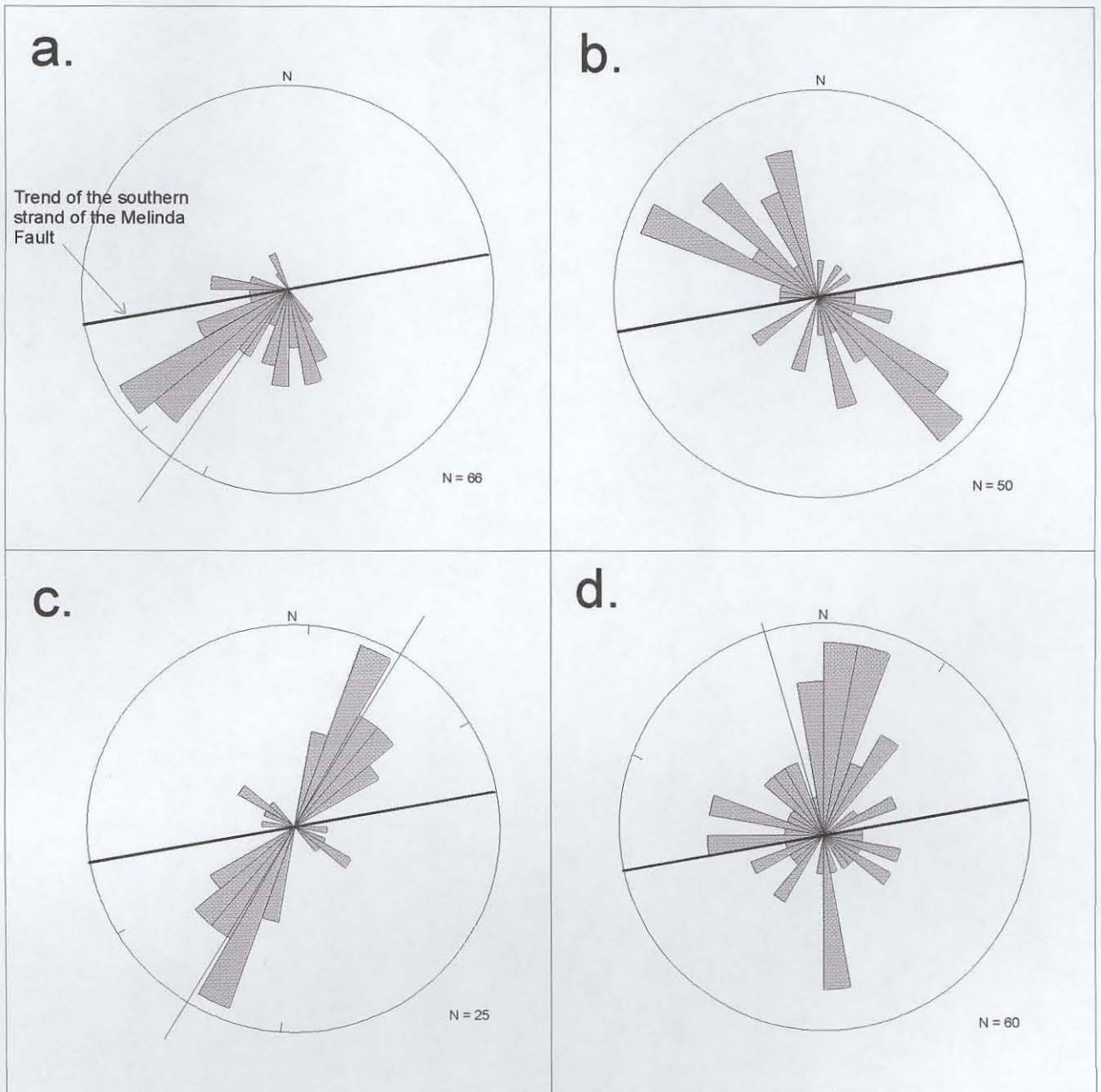


Figure 5.17: Photomicrograph from a sandstone pebble within the Wyllies Poort Formation. Sub-angular quartz grains are supported by interstitial red clay minerals.



**Figure 5.18: Photomicrograph of coarse sandstone from the Mogalakwena Formation, showing sub-angular quartz grains with interstitial red clay minerals. c.f. Figure 5.17.**



**Figure 5.19: Rose diagrams showing the palaeocurrent directions recorded in different facies of the Wyllies Poort Formation: a.) Trough cross-bedded sandstone; b.) Asymmetric ripplemarks; c.) Symmetric ripplemarks (trend); d.) Asymmetric Ripplemarks in north-eastern foothills of Blouberg. Where appropriate, principal direction (vector mean) is indicated.**



%	175	177	208
SiO <sub>2</sub>	49.05	50.84	48.56
TiO <sub>2</sub>	1.27	0.93	1.96
Al <sub>2</sub> O <sub>3</sub>	13.45	14.13	14
Fe <sub>2</sub> O <sub>3</sub>	13.8	11.83	16.31
MnO	0.18	0.18	0.21
MgO	3.59	6.25	5.42
CaO	12.12	9.33	6.92
Na <sub>2</sub> O	0.16	1.95	3.83
K <sub>2</sub> O	3.68	1.49	0.048
P <sub>2</sub> O <sub>5</sub>	0.14	0.09	0.25
Cr <sub>2</sub> O <sub>3</sub>	0	0.01	0.02
NiO	0.01	0.02	0.01
LOI	1.44	2	2.54
<b>Total</b>	<b>98.97</b>	<b>99.12</b>	<b>100.62</b>
Cu	98	101	249
Ga	27	17	20
Mo	2	<1	<1
Nb	9	6	8
Ni	80	141	82
Pb	5	3	2
Rb	101	62	13
Sr	412	255	260
Th	<5	<5	<5
U	<3	<3	<3
Y	33	22	40
Zn	81	84	137
Zr	142	104	177
Ba	223	404	358
Cl	32	<30	<30
Cr	27	60	130
%S	<0.01	<0.01	<0.01
Sc	38	31	35
V	312	230	384

Element	175	177	208
La	20.3	15.5	19.6
Ce	41.0	32.8	45.0
Pr	5.22	3.96	5.55
Nd	21.3	16.1	24.1
Sm	4.66	3.47	5.64
Eu	1.32	1.01	1.62
Gd	4.59	3.63	6.31
Tb	0.77	0.58	1.04
Dy	4.91	3.63	6.79
Ho	1.00	0.71	1.40
Er	2.91	1.97	4.02
Tm	0.41	0.28	0.57
Yb	2.63	1.81	3.75
Lu	0.38	0.27	0.57
Nb	9.0	6.0	8.0

**Table 5.1: X.R.F and I.C.P.M.S. results for major (%) and trace (ppm) element abundances in the Sibasa Formation. Sample 175 is from 23° 06.73'S; 28° 47.61'E. Sample 177 is from 23° 07.10'S; 28° 50.10'E. Sample 208 is from 23° 07.30'S; 28° 54.70'E.**